

# Comparison of Hydrodynamic, Energy and Exergy Efficiency of Two-phase Hybrid Nanofluid in Parabolic Trough Solar Collector with Vortex Generator and Turbulator

Ali Golzar<sup>1</sup>, Alireza Aghaei<sup>2\*</sup>, Hamid Mohseni Monfared<sup>1</sup>, Ali Hassani Joshaghani<sup>3</sup>

<sup>1</sup> Department of Mechanical Engineering, Arak Branch, Islamic Azad University, Arak, Iran

<sup>2</sup> Department of Mechanical Engineering, University of Kashan, Iran

<sup>3</sup> Department of Chemical Engineering, Arak Branch, Islamic Azad University, Arak, Iran

**ABSTRACT:** The present study follows a 3D modeling of the geometry of a parabolic trough solar collector (PTSC) equipped with a twisted cross turbulator (TCT) and a Vortex Generator with Pitch Ratio (VGPR), considering the finite volume method (FVM) to solve the governing equations. The absorber tube (AT) of this PTSC is equipped with a TCT and a VGPR in order to increase thermal performance (TP). Also, the efficiency of their use on different output parameters have been compared. In addition, in order to be more practical, the efficiency of the geometric shape of the TCT and VGPR on various parameters in the output has been investigated. In order to make the study more practical, graphene oxide (GO) and double-walled carbon nanotubes (DWCNT) nanoparticles (NP) are dispersed in the base fluid (BF). The study is conducted at high Reynolds numbers (Re) (from 15,000 to 60,000), corresponding to the turbulent regime's range. Numerical simulation results show that the velocity change in the AT is a positive factor in all cases of increase. Because in all these cases, the increase of this parameter has caused the average Nusselt number ( $Nu_{ave}$ ) to rise. Also, Syltherm 800 (BF) has a lower thermal conductivity (k) coefficient than hybrid nanofluid (HNF) Syltherm 800/DWCNT- GO, resulting in lower TP in PTSC. The addition of TCT, VGPR, and their geometrical change has a positive role in the hydrodynamic behavior of Syltherm 800/DWCNT-GO HNF flow. In all geometric modes, the PEC index is more significant than one, so using these two mechanical parts always has a better TP than the pressure drops ( $\Delta P$ ) resulting from their presence. Finally, by examining the exergy efficiency ( $\eta_{ex}$ ), It was observed that the maximum practical work received from the solar system (SS) was obtained when using the VGPR in the flow path of HNF Syltherm 800/DWCNT-GO.

**KEYWORDS:** Parabolic trough solar collector, Vortex generator, Twisted cross turbulator, Turbulent flow, Two-phase flow, Hybrid nanofluid

## INTRODUCTION

Energy sources can be divided into two categories: renewable and non-renewable. Renewable energy sources include solar, geothermal, wind, biomass, and hydroelectric energy. These energy sources are called renewable energies because they are naturally replaced again. Today, solar technologies can use this energy for various purposes, including generating electricity, lighting a comfortable interior, and heating H<sub>2</sub>O for domestic, commercial, or industrial use. Göksu and Behçet [1] experimentally studied and investigated the efficiency of using a vortex generator (VG) on energy efficiency ( $\eta_{en}$ ) and  $\eta_{ex}$  in a heat exchanger (HE). This research was conducted in a reliable laboratory system with international standard devices. The results indicate that adding a VG increase  $\eta_{en}$  and decreases  $\eta_{ex}$  at high Re. The  $\eta_{en}$  in this study has increased up to 31.60% due to the use of the torsion VG. In a two-dimensional numerical investigation, Parsaiemehr et al. [2] studied the efficiency of cylindrical teeth on the wall of a channel. This study has been done considering double accuracy in numerical simulation. The results of this study state that the presence of cylindrical teeth on the channel wall affects the outlet temperature in the channel. When the outlet

temperature is affected, the heat transfer (HT) naturally increases, and as a result, the TP of the channel increases. Jalalian Larki et al. [3] studied the efficiency of phase change material and VG in a thermal system. The study has been carried out with the assumptions of slow, stable, and incompressible flow. Using phase change materials in the heating system has increased TP. Nevertheless, using a VG and increasing the TP has caused a significant  $\Delta P$  in the thermal system. The authors state that phase-change materials can increase HT by 29.74%. Jassim and Ahmed [4] investigated the environmental and thermal efficiency caused by the presence of a VG in a flat plate HE. This study places the VG in the center of the flat plate HE and the nanofluid (NF) flow path. In this study, titanium oxide and aluminum oxide NP have been used in oil BF. It can be concluded that the ambient temperature results in the flat plate HE is more favorable when using the VG and NF because the output results show that in this mode, the amount of carbon dioxide output from the flat plate HE is lower than in other modes. Sun et al. [5] studied and investigated the efficiency of using VG with curtain rotation on  $\eta_{ex}$  and thermal efficiency in a HE experimentally and numerically.

\* Corresponding author's email: [a.aghaei@kashanu.ac.ir](mailto:a.aghaei@kashanu.ac.ir)  
Tel.: +983155338222

<b>Nomenclature</b>			
$D$	diameter of receiver	$\varepsilon$	Turbulent dissipation rate
$GO$	Graphene oxide	$k$	Turbulent kinetic energies
$h$	Heat transfer coefficient (W/m <sup>2</sup> K)	<b>subscripts</b>	
$K$	Thermal conductivity (W/m·K)	$bf$	Base fluid
$L$	Length (mm)	$nf$	nanofluid
$DWCNT$	double-walled carbon nanotubes	$np$	nanoparticle
$Nu$	Nusselt number	$f$	fluid
$NFs$	Nanofluids	$s$	solid
$NPs$	Nanoparticles	<b>Abbreviations</b>	
$P$	Pressure (Pa)	$PTSC$	Parabolic trough solar collector
$T$	Temperature (°C)	$TCT$	Twisted cross turbulator
$Re$	Reynolds number	$VGPR$	Vortex Generator with Pitch Ratio
$V$	Velocity (m/s)	$HNF$	Hybrid Nanofluid
$\Delta P$	Pressure drop	$TP$	Thermal performance
<b>Greek symbol</b>		$FVM$	Finite volume method
$\phi$	Volume concentration (%)	$PEC$	Performance evaluation criteria
$\mu$	Dynamic Viscosity (cP)	$AT$	Absorber tube
$\rho$	Density (kg/m <sup>3</sup> )	$SS$	solar system

In this study, VG with curtains was modeled with different geometric states of the number of blades. Also, the studied geometry has been analyzed in three dimensions, and the vortex of rotating VG has been placed in the middle part of the inner tube of the HE in the fluid flow path. According to the reports of the output  $\eta_{ex}$  values, increasing the number of blades can benefit Newton's second law at low Re. Therefore, with the increase of Re, the  $\eta_{ex}$  decreases. Also, the increase in the number of blades causes positive changes in the TP of the system they studied. Abidi et al. [6] studied the geometrical design of a twisted tape (TT) to improve thermal efficiency in a PTSC. In this SS, Water/copper oxide NF is flowing. By examining the graphs presented in their output, it can be concluded that the  $\eta_{ex}$  values grow significantly due to the addition of the TT to the PTSC. This study's turbulent kinetic energy changes indicate that the TT causes changes in the base under the viscous layer and is formed by rotating vortices.

In a numerical study, Sheikholeslami et al. [7] investigated the efficiency of TT geometry combined with surface blades on  $\eta_{ex}$  and  $\Delta P$  in a PTSC. The ratio of the pitch, thickness, and rotation of the TT combined with the surface blades have been investigated in this study, and their changes have been reported in terms of  $\eta_{ex}$  and  $\Delta P$ . This study's output results show that the PTSC's  $\Delta P$  in the presence of the TT combined with surface blades is very high. Nevertheless, the PEC index states that using a TT combined with surface blades is desirable. The maximum  $\eta_{ex}$  in this study is 20.73%. Modi et al. [8] investigated the efficiency of using needle teeth on entropy production and  $\eta_{en}$  in a HE with an elliptical cross-section in a two-dimensional way. Investigating the efficiency of needle

teeth, considering the amount of  $\Delta P$  and HT caused by them, is one of the main goals of this study. The study has been carried out with the assumptions of turbulent, permanent, and incompressible flow. The results show that entropy production and  $\eta_{en}$  values decrease and increase, respectively, in the presence of needle teeth. The maximum  $\eta_{en}$  increase in this study was reported to be 40.11%. Sharma et al. [9] numerical simulation of a two-dimensional channel containing H<sub>2</sub>O -iron oxide NF under the influence of a rotating magnetic field. Their study has been done in a slow, permanent, and incompressible flow regime. In addition, the double precision solution has been used in the research to have accurate results and optimal convergence. By examining the output graphs, it can be stated that the use of magnetic NP and their application caused the NF flow to become a vortex in the middle of the channel. In addition, applying magnetic force positively affects the HT process in the channel geometry. Ye et al. [10], a microchannel equipped with internal fins was investigated numerically using CFD. In order to investigate the environment in this study, the efficiency of using H<sub>2</sub>O -aluminum oxide NF and H<sub>2</sub>O have been compared with each other. By examining the diagrams presented in this study, it can be concluded that the geometrical change of internal fins is significant in the change of hydraulic and thermal parameters. Also, the environmental analysis shows that when using the H<sub>2</sub>O -aluminum oxide NF, the amount of environmental pollution caused by the release of carbon dioxide in the microchannel is less than when the working fluid is H<sub>2</sub>O.

In a numerical study, Kumar and Hiremath [11] investigated the efficiency of propeller-shaped VG on entropy production inside a microchannel with a rectangular cross-section. The study has investigated different heights of

propeller-shaped VG wings. The results of this study show that the higher the height of the VG wing, the more the fluid flow rotates after hitting it, resulting in higher TP. Nevertheless, this study's results show that the  $\Delta P$  increase is almost 1.5 times higher than TP. Liang et al. [12] analyzed a microchannel equipped with needle-shaped TT using response surface methodology. Also, this study presents a theoretical relation to estimating the  $Nu_{ave}$  for predicting fluid flow behavior using the artificial neural network method. The results obtained from this study show that the diameter of the needle TT is directly related to the HT coefficient in the microchannel. In fact, with the increase in the diameter of the needle TT, the displacement transfer coefficient increases to a maximum of 60.82%. In a numerical study, Sheikholeslami et al. [13] investigated the behavior of an HNF in a PTSC around a rotating TT. This study investigated the rotary TT's width, thickness, and pitch ratio parameters. The authors present the obtained values for  $\eta_{ex}$  in each geometric state for different Re in a volume fraction ( $\phi$ ) 1% of an HNF. The reports state that the  $\eta_{ex}$  has an upward performance only at low Re. Because the amount of work available from the system decreases with the increase of Re. Al-Rashed et al. [14], in a study based on CFD, the changes in the geometric shape of the cylindrical fins on the wall of the AT of the PTSC were investigated. This study uses a computer code to model the solar heat flux. The study is reviewed for 12 months of the year. With the interpretation of the presented output, it can be stated that the output temperature is much higher in the hot seasons of the year. Because in these seasons, the intensity of solar radiation is high, and as a result, the output temperature will be higher. Also, by examining the flow behavior around the fins, the closer the fins are to each other, the higher the HT at the collector's output. Bellos et al. [15] investigated the changes  $\eta_{ex}$  and environmental efficiency in the presence of a strip TT and NF. In this study, the constant heat flux corresponding to the average annual radiation of Greece is used to model solar radiation. The geometry of the TT is placed in the center of the PTSC and the flow path of the H<sub>2</sub>O -copper oxide NF. The output results show that  $\eta_{en}$  and  $\eta_{ex}$  up to Re = 7000 have similar and increasing performance. Nevertheless, with the increase of Re, the values of B increase, and  $\eta_{ex}$  decreases. Also, the amount of carbon dioxide in the output of the PTSC is lower when using H<sub>2</sub>O -copper oxide NF. Gururatana et al. [16] the efficiency of the pitch ratio of a VG in a thermal system was analyzed. The efficiency of the pitch ratio, thickness, and transverse ratio on the geometry of the VG has been investigated in this study. The presented reports show that the fluid flow after hitting the VG of the areas has undergone rotational movement, which is one reason for creating the vortex. Also, changing the geometric parameters and increasing them in the HT process has shown positive efficacy. Zheng et al. [17] the hydraulic-thermal study of a two-pipe converter with VG with different geometric shapes. In this study, the

acceleration of Earth's gravity has been considered. Due to the accuracy of the calculations and the high-temperature gradient, an excellent grid has been used in the areas close to the wall. The efficiency of a VG with three pyramidal, cylindrical, and square geometry shapes has been investigated. The results indicate that the VG with the pyramidal congress creates the highest thermal efficiency in the double-tube converter. Berber and Gürdal [18] used the artificial neural network method to investigate the efficiency of using rectangular ribs with different geometric shapes in a rectangular channel. This study presents a theoretical relationship to estimate HT in a rectangular channel. The numerical results presented in this research show the high growth of  $\Delta P$  caused by rectangular ribs in the channel. The excessive increase in  $\Delta P$  has made using this geometric shape of ribs unsuitable for thermal hydraulics. Lu et al. and Zhai [19] studied the efficiency of using blade VG with different geometric modes on TP and  $\eta_{ex}$  in an HE with an elliptical inner tube. The efficiency of thickness, height, and vortex length of blade VG have been analyzed in this study. According to the reports provided by the authors, by changing all three geometric parameters of height, thickness, and length, the values of HT,  $\Delta P$ , and  $\eta_{ex}$  increase significantly. Therefore,  $\eta_{ex}$  values increase up to Re = 6000 and then decrease. Nevertheless, the values of HT and  $\Delta P$  are constantly increasing with the increase of HT. Nikoozadeh et al. [20] investigated and studied the efficiency of a propeller TT with a combined geometric shape on HT and  $\eta_{ex}$  in a tube containing H<sub>2</sub>O -aluminum oxide NF. In this study, excellent mesh is used in the areas near the TT and the walls to increase the accuracy of the calculations. Also, the governing equations of the problem have been solved using double precision. All Re averaging models have been compared to transfer the turbulence model in this study. According to the results presented by the authors, the propeller TT helps change the flow form and the amount of turbulence at high Re. This causes the formation of vortices. Mohammed et al. [21] investigated the efficiency of using HNF and conical TT in PTSC on TP and  $\eta_{ex}$ . The studied HNF has been modeled with silver NP, multi-walled carbon nanotubes, and magnesium oxide in different states. Also, the influence of the ratio of width, height, and thickness of the TT has been analyzed. The reports presented in this study indicate that the HNF with silver and multi-walled carbon nanotubes has better TP than the rest of the compounds. Also, placing the conical TT in the PTSC will increase the SS efficiency in terms of the newton second law.

Using the artificial neural network method, Fuxi et al. [22] investigated the HNF flow behavior around a spiral TT in a PTSC. This study presented a theoretical relationship to predict the flow behavior of H<sub>2</sub>O -titanium oxide-copper NF in a PTSC. The amount of solar radiation in their study was chosen based on the average annual radiation in China. By examining the results presented in their research, it can be stated that the HNF rotates after encountering the spiral TT,

and vortices are formed around it. The number of changes in TP due to the presence of a HNF is reported as 12.74%. Alqaed et al. [23] using the artificial neural network method, they investigated the efficiency of a spiral TT on  $\eta_{en}$  and  $\eta_{ex}$  in a PTSC containing a HNF. The studied HNF consists of aluminum and copper oxide NP with an average diameter of 40 to 70 nm. The PTSC has been investigated in non-uniform heat flux for 6 hours daily. The results of this research show that  $\eta_{en}$  and  $\eta_{ex}$  values increase with input speed changes. In the areas close to the TT, continuous flow lines change due to the creation of swirling flow. Song et al. [24] placing cylindrical fins increased the hydraulic-thermal efficiency in a HE. This study analyzed thermal-hydraulic efficiency by changing the angle between cylindrical fins. The angle of the fins in their study has been changed between 20 and 50 degrees. The authors' statements show that the HT and the angle of change of the fins are directly related. In this way, if the angle of the fins increases, the HT will also increase. In addition, as a negative factor, fins increase the  $\Delta P$ . Of course, its values are significant compared to the increase in HT.

Aghaei et al. [25] modeled a PTC in the turbulent flow regime using the computational fluid dynamics technique. This study aimed to investigate the volume fraction of nanoparticles, turbulent flow, and increase in the inlet velocity on the values of energy efficiency, exergy, and PEC index in the PTC. Based on the presented results, this study's amount of PEC index has favorable changes in all modes. Pour Razzaghi et al. [26] investigated the effects of a magnetic field and twisted turbulator in a PTC. This study uses the finite volume method and Fluent software to solve the problem. In addition, in the whole study, the assumption of turbulent flow is considered for modeling. Also, the K-Omega turbulence model has been used for viscosity modeling. The results show that the simultaneous application of magnetic field and twisted turbulator increases the thermal efficiency and friction coefficient values in the PTC by 46.26% and 70.01%, respectively. Roohi et al. [27] investigated the simultaneous effect of Helical Screw Tape and nanofluid on the thermal performance of a PTC. In this study, the effect of volume fraction of 1 to 3% of nanofluid and different twist ratios of Helical Screw Tape on thermal performance and PEC index in PTC has been investigated. According to the obtained results, the long-term use of Helical Screw Tape and nanofluid had a positive role on the thermal performance of the PTC. Also, PEC index values have increased by 3.12% when using Helical Screw Tape. Dezfulizadeh et al. [28] designed a new geometry of the twisted turbulator to increase the thermal efficiency in the PTC. In this study, the criteria for designing the appropriate geometrical shape of the twisted turbulator have been determined using the results of the PEC index. In this study, the assumption of turbulent and stable flow is considered for numerical modeling. The output results show that the thermal efficiency of the PTC increases by 58.23% in the best case. Esmacili et al. [29] investigated the effect of

twisted turbulators and hybrid nanofluids in different volume fractions inside a PTC. In this study, the assumption of steady and turbulent flow is used. Also, for numerical simulation, Fluent software and finite volume method have been used. The results presented in this study show that the amount of heat transfer has increased by 35.7%. Abidi et al. [30] numerically investigated the efficiency of non-uniform heat flux in this PTSC containing magnetic NF and twisted TT. In this study, a computer code on the surface of the AT has applied non-uniform heat flux for 12 months and 7 hours of work per day. In order to increase the accuracy of calculations, the double precision solution has been used. Magnetic NP have been used due to their high  $k$  compared to the BF. The reports presented in their research show that with the growth of the  $\phi$  of NP, the values of the  $Nu_{ave}$  find an upward trend. Also, according to the results, the maximum outlet temperature is related to the summer season. Jafaryar et al. [31] investigated the comparison of HNF and combined TT on the TP of PTSC in the turbulent flow regime. This research investigated the efficiency of HNF and TT on the output values of displacement HT coefficient and friction coefficient. Also, in order to reduce computational costs, constant heat flux has been used to model solar radiation. The values presented in the output show that the combined TT creates more TP in the PTSC output than the NF. Also, the conducted investigations state that if these two parameters are placed simultaneously in the PTSC, they can increase the HT by 63.11%. Optimizing heat transfer is a priority in all industries, especially engineering ones. Increasing displacement heat transfer by mixing nanoparticles with different materials in base fluids has recently been especially welcomed by researchers [32-34]. These characteristics have caused nanofluids to be used in various industries as coolants, lubricants, and hydraulic fluids [35, 36].

Table 1 compares the relationship and difference of the present study with other studies conducted in the field of parabolic solar collectors. As mentioned in the separate review of each of the studies, the purpose of using the turbulator or vortex generator is to increase the thermal efficiency of the PTSC. As mentioned in Table 1, the geometric shape of the turbulator and vortex generator is different in each study. Choosing a geometric shape is a matter of taste and according to the opinions of researchers and scientists. However, considering that using a turbulator can negatively affect pressure drop and increase pumping power, the main goal of this study is to design the geometry of a PTSC equipped with a turbulator and vortex generator, considering energy optimization and logical pressure drop. In addition, as shown in Table 2, none of the studies compared the effects of vortex generators and turbulators. This is while the present study examines and compares the effect of vortex generators and turbulator separately. In addition, the hybrid nanofluid is modeled in the present study by considering the two-phase model.

**Table 1.** Comparison of the present study with studies conducted in the field of PTSC

Reference	Methods	Nanofluid type	Modeling nanofluid	Geometric shape of vortex generator or turbulator
Abidi et al. [6]	CFD analysis	CuO/Water	Single-phase method	Twisted tape with circular holes
Sheikholeslami et al. [7]	CFD analysis	SiO <sub>2</sub> -CNT/Water	Single-phase method	Fins with horseshoe shape
Sheikholeslami et al. [13]	CFD analysis	Al <sub>2</sub> O <sub>3</sub> -CuO/Water	Single-phase method	Helical coil and twisted tape
Alqaed et al. [23]	CFD analysis	TiO <sub>2</sub> -Cu/Water	Single-phase method	Spring turbulator
Jafaryar et al. [31]	CFD analysis	Al <sub>2</sub> O <sub>3</sub> -MWCNT/Oil	Single-phase method	Multi helical tapes
Shaker et al. [37]	CFD analysis	Al <sub>2</sub> O <sub>3</sub> /Syltherm	Single-phase method	flange-shaped turbulator
Present study	CFD analysis	DWCNT-GO/ Syltherm 800	Two-phase method	Twisted cross turbulator and Vortex Generator

As mentioned in previous studies, the geometric shape of the turbulator and vortex generator is different in each study. Choosing a geometric shape is a matter of taste and according to the opinions of researchers and scientists. However, considering that using a turbulator can negatively affect pressure drop and increase pumping power, designing a suitable geometry with reasonable pressure drop is always considered necessary. The main goal of the present study is to design the geometry of the solar collector equipped with a turbulator and vortex generator, considering energy optimization and reasonable pressure drop. In addition, the effects of using the vortex generator and turbulator with the geometric shape of the present study have not been investigated by any researcher. Also, as mentioned in previous studies, researchers use a single-phase method for nanofluid modeling. Therefore, two-phase modeling of Syltherm 800/DWCNT-GO hybrid nanofluid in 2% and 4% volume fractions has not been investigated so far. The present study follows a three-dimensional modeling of the geometry of a PTSC equipped with TT and VG, considering the FVM to solve the governing equations. The AT of this PTSC is equipped with TT and VG to increase TP. Also, the efficiency of their use on different output parameters has been compared. In addition, to be more practical, the efficiency of the geometric shape of the TT and VG on various parameters in the output has been investigated. In order to make the study more practical, GO and DWCNT NP are dispersed in this BF. The study is conducted at high Re

(15,000 to 60,000), corresponding to the turbulent regime range.

### The Studied SS and Its Governing Equations PTSC with VGPR and TCT

Using solar energy as an alternative to fossil fuels brings significant achievements for humanity and engineering industries worldwide. In better words, although fossil fuels can still be used with limited resources, there is an endless source of sunlight, which is the source of solar energy. Also, solar energy does not cause pollution like burning fossil fuels. On the other hand, increasing the efficiency of SS has attracted the attention of researchers and various industries. Therefore, according to these issues, the increase in thermal efficiency in the present study is investigated in the PTSC. The PTSC system in the present study is presented schematically in Fig. 1. As shown in the figure, the AT of this PTSC is equipped with a VGPR and TCT in order to increase TP. In addition, in order to be more practical, the efficiency of the geometric shape of the VGPR and TCT on various parameters in the output has been investigated and compared with each other. Syltherm 800 HT oil, combines excellent thermal stability and low viscosity for reliable and consistent performance in a single system. In this study, this oil was used as the BF. Also, since this fluid has a low  $k$ , to make the study of GO and DWCNT NP more practical, they are dispersed in this BF. The study is conducted at high Re (from 15,000 to 60,000), corresponding to the turbulent regime's range.

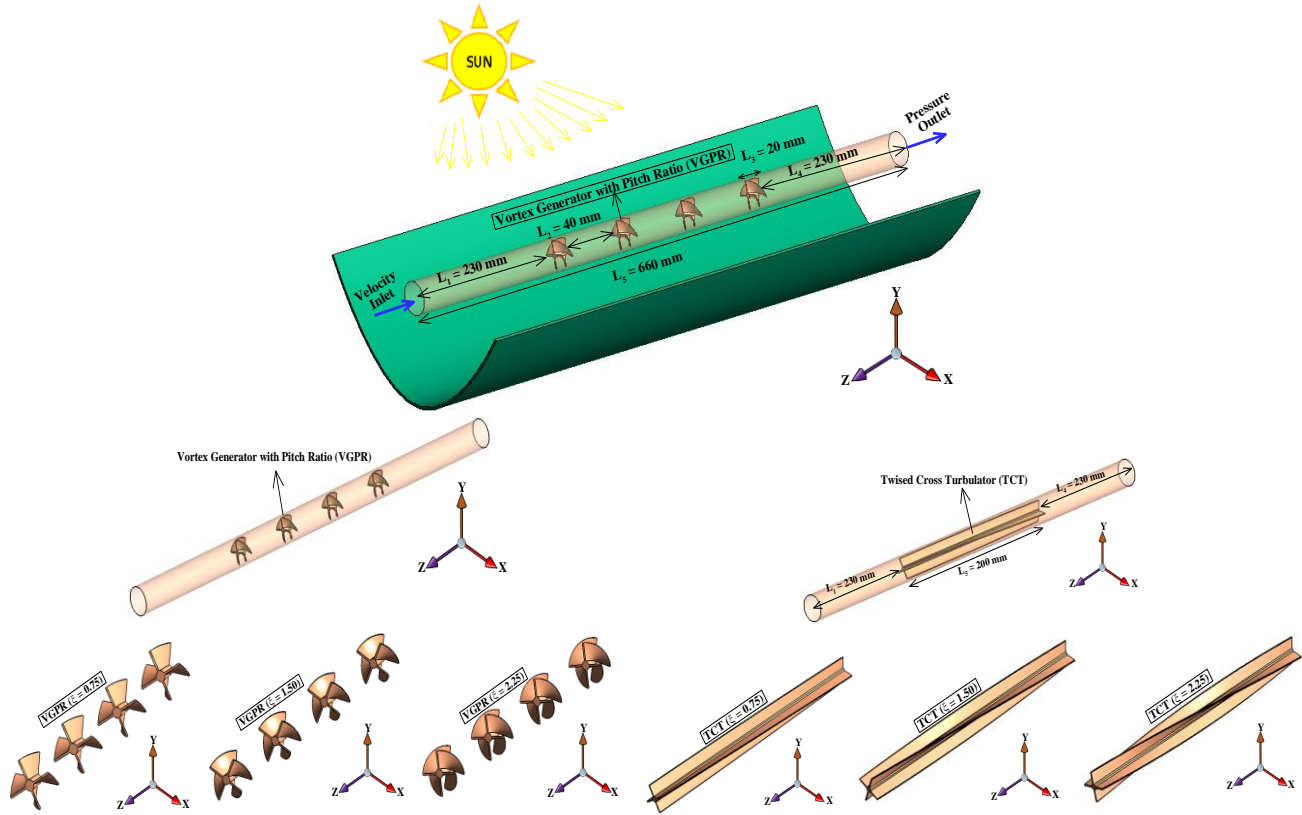


Fig. 1. Schematic of the studied SS

### Numerical Modeling and HNF

In this study, Ansys Fluent software was used for numerical modeling. Fig. 2 describes the boundary conditions and how Fluent software sets the numerical solution. The AT of this PTSC is equipped with TCT and VGPR in order to increase TP. Also, the efficiency of their use on different output parameters have been compared. In addition, in order to be more practical, the efficiency of the geometric shape of the TCT and VGPR on various parameters in the output has been investigated. In order to make the study more practical, GO and DWCNT NP are dispersed in this BF. The study is

conducted at high Re (from 15,000 to 60,000), corresponding to the turbulent regime's range. Also, in order to model the turbulent flow, the Realizable k-ε turbulence model has been used. After determining the turbulence model, the height of the first cell of the boundary layer should be determined. The height of the first cell of the boundary layer depends on factors such as viscosity, the length of the viscous region, fluid velocity, density, and, most importantly, the  $Y^+$  value. Enhance wall treatment was used in this study. Therefore,  $Y^+ < 5$  should be considered [38].

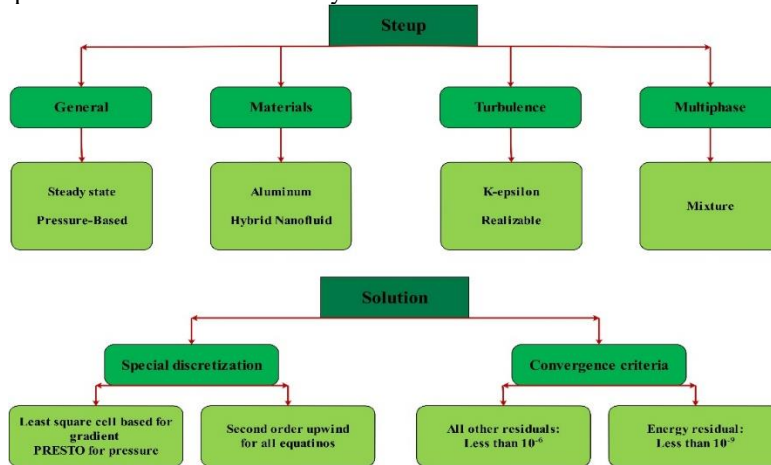


Fig. 2. FLUENT set up details

To model the HNF, we must first have the thermophysical properties of the NP used in the NF. In this study, GO and DWCNT NP were used. The thermophysical properties of NP are reported in Table 2. As mentioned, this study is carried out with the assumption of dispersing GO and DWCNT NP in Syltherm 800 oil-based fluid. Reference [49] is used to calculate the thermophysical properties of this BF. It should be noted that this BF is a synthetic oil with stable characteristics at high temperatures. Finally, relations

$$\rho_{HNF} = \rho_{GO}\phi_{GO} + \rho_{DWCNT}\phi_{DWCNT} + \rho_{Syltherm\ 800}(1 - \phi_{GO} - \phi_{DWCNT}) \quad (1)$$

$$(c_p)_{HNF} = (c_p)_{GO}\phi_{GO} + (c_p)_{DWCNT}\phi_{DWCNT} + (c_p)_{Syltherm\ 800}(1 - \phi_{GO} - \phi_{DWCNT}) \quad (2)$$

$$\mu_{HNF} = \mu_{Syltherm\ 800}(1 - \phi_{GO} - \phi_{DWCNT})^{-2.5} \quad (3)$$

$$k_{HNF} = k_f \left( \frac{(k_{GO} + k_{DWCNT}) + 2k_{Syltherm\ 800} - 2\varphi_{GO}(k_{Syltherm\ 800} - k_{GO}) - 2\varphi_{DWCNT}(k_{Syltherm\ 800} - k_{DWCNT})}{(k_{GO} + k_{DWCNT}) + 2k_{Syltherm\ 800} + \varphi_{GO}(k_{Syltherm\ 800} - k_{GO}) + \varphi_{DWCNT}(k_{Syltherm\ 800} - k_{DWCNT})} \right) \quad (4)$$

### Governing Equations of the Studied SS

The simulation of two-phase model (TPM) and multiphase flows in Fluent is increasingly important in engineering. TPM has different methods, each of which is different according to the physics of the problem. The mixture model in AnasysFluent is designed for two or more phases. In a mixture model like the Eulerian model, phases can be intertwined. The mixture model is usually used for NF modeling. Because in this model, the phases are considered a continuous interpenetrating medium, the momentum equations are solved for the mixture, and the relative velocities are used to describe the dispersed phases. The governing equations of the PTSC system equipped with the VGPR containing TPM DWCNT- GO /Syltherm 800 are rewritten below [43, 44]. It is possible to calculate the inlet velocity in the parabolic solar collector using the Reynolds number relation (Eq. 16) [45]. In this relation,  $\vec{U}_m$  is the inlet velocity,  $d_p$  is the diameter of the absorber tube of the solar collector,  $\rho_{HNF}$  is the density, and  $\mu_{HNF}$  is the viscosity of the hybrid nanofluid. In addition, the pressure drop in the parabolic solar collector can be calculated using equation 17. In this relationship,  $P_{av,inlet}$  is the inlet pressure, and  $P_{av,outlet}$  is the outlet pressure. Also, the average Nusselt number and thermal-hydraulic performance coefficient can be calculated using Eqs. 18 and 19, respectively.

$$\nabla(\rho_m \vec{U}_m) = 0 \quad (5)$$

$$\vec{U}_m = \frac{\rho_s \phi_s \vec{U}_s + \rho_{bf} \phi_{bf} \vec{U}_{bf}}{\rho_m} \quad (6)$$

$$\rho_m = \rho_s \phi_s + \rho_{bf} \phi_{bf} \quad (7)$$

$$\rho_m (\vec{U}_m \nabla \vec{U}_m) = -\nabla \vec{P} + \mu_m (\nabla \vec{U}_m + (\nabla \vec{U}_m)^T) + \nabla(\rho_{bf} \phi_{bf} \vec{U}_{dr,bf} \vec{U}_{dr,bf} + \rho_s \phi_s \vec{U}_{dr,s} \vec{U}_{dr,s}) + \rho_m \vec{g} \quad (8)$$

$$\vec{U}_{dr,bf} = \vec{U}_{bf} - \vec{U}_m \quad (9)$$

$$\vec{U}_{dr,s} = \vec{U}_s - \vec{U}_m \quad (10)$$

1 to 4 are used to calculate the thermophysical properties of HNF GO -DWCNT/ Syltherm 800 [40].

**Table 2.** Characteristics of NP [41, 42]

Nanoparticle	$\rho$ ( $kg \cdot m^{-3}$ )	$c_p$ ( $Jkg^{-1}K^{-1}$ )	$k$ ( $W \cdot m^{-1} \cdot K^{-1}$ )
DWCNT	2100	519	3000
GO	1910	710	1000

$$\nabla(\rho_{bf} \phi_{bf} \vec{U}_{bf} h_{bf} + \rho_s \phi_s \vec{U}_s h_s) = \nabla((\phi_{bf} k_{bf} + \phi_s k_s) \nabla \vec{T}) \quad (11)$$

$$\nabla(\rho_s \phi_s \vec{U}_m) = -\nabla(\rho_s \phi_s \vec{U}_{dr,s}) \quad (12)$$

$$\vec{U}_{bf,s} = \vec{U}_{bf} - \vec{U}_s \quad (13)$$

$$\vec{U}_{dr,s} = \vec{U}_{s,bf} - \frac{\rho_s \phi_s}{\rho_m} \vec{U}_{bf,s} \quad (14)$$

$$\vec{U}_{bf,s} = \frac{d_p^2}{18\mu_{bf} \mathcal{f}_d} \frac{\rho_s - \rho_m}{\rho_s} \vec{a} \quad (15)$$

$$\mathcal{f}_d = 1 + 0,15Re_s^{0,687}$$

$$\vec{a} = \vec{g} - (\vec{U}_m \nabla \vec{U}_m)$$

$$Re_s = \frac{\vec{U}_m d_p \rho_m}{\mu_m} \quad (16)$$

$$\nabla(\rho_m \vec{U}_m k) = \nabla \left[ \left( \mu_m + \frac{\mu_{t,m}}{\sigma_k} \right) \nabla k \right] + G_{k,m} - \rho_m \varepsilon \quad (17)$$

$$\nabla(\rho_m \vec{U}_m \varepsilon) = \nabla \left[ \left( \mu_m + \frac{\mu_{t,m}}{\sigma_\varepsilon} \right) \nabla \varepsilon \right] + \frac{\varepsilon}{k} (c_1 G_{k,m} - c_2 \rho_m \varepsilon)$$

$$\mu_{t,m} = C_\mu \rho_m \frac{k^2}{\varepsilon} \quad (18)$$

$$G_{k,m} = \mu_{t,m} (\nabla \vec{U}_m + (\nabla \vec{U}_m)^T) \quad (19)$$

$$Re_{HNF} = \frac{\vec{U}_m d_p \rho_{HNF}}{\mu_{HNF}} \quad (20)$$

$$\Delta P = P_{av,inlet} - P_{av,outlet} \quad (21)$$

$$Nu = \frac{h_{HNF} \cdot D_i}{k_{HNF}} \quad (22)$$

$$PEC = \left( \frac{Nu_{av\&HNF\&VGPR\&TCT}}{Nu_{av\&HNF\&Without\ VGPR\ and\ TCT}} \right) \cdot \left( \frac{\Delta P_{HNF\&VGPR\&TCT}}{\Delta P_{HNF\&Without\ VGPR\ and\ TCT}} \right)^{-1/3} \quad (23)$$

$$\eta_c = \frac{E_c}{I \cdot A} = \frac{Q_{in} \cdot \rho_{in} \cdot c_{p,in} \cdot (T_{out} - T_{in})}{6 \cdot 10^4 \cdot I \cdot A} \quad (24)$$

$$\eta_n = \frac{E_n}{I \cdot A} = \frac{p_{fo} \cdot Q_{in} \cdot \rho_{in} \cdot c_{p,in} \cdot (T_{fo,out} - T_{in}) + (1 - p_{fo}) Q_{in} \cdot \rho_{in} \cdot c_{p,in} \cdot (T_{f,out} - 7)}{6 \cdot 10^4 \cdot I \cdot A} \quad (25)$$

$$E_u = Q_u - \dot{m} c_p T_0 \ln \left( \frac{T_{outlet}}{T_{inlet}} \right) \quad (26)$$

$$E_s = Q_s \left[ 1 - \frac{4}{3} \left( \frac{T_0}{T_{sun}} \right) + \frac{1}{3} \left( \frac{T_0}{T_{sun}} \right) \right] \quad (27)$$

$$\eta_{ex} = \frac{E_u}{E_s} \quad (28)$$

### Grid Independency and Validation

#### Grid Independency

To check the optimal grid in the studied SS, the output values obtained from the  $Nu_{ave}$  for the network with different points have been investigated. This review is for the case where the PTSC is equipped with a TCT and a VGPR ( $\xi = 2.25$ ,  $\phi = 4\%$ , and  $Re = 60000$ ) has been done. Not checking the grid independency is one factor leading to wrong results in CFD. Therefore, this process should be done in at least several steps in each type of simulation. This makes you more confident in your results. The results of the  $Nu_{ave}$  for PTSC equipped with TCT and VGPR are presented in Fig. 3 and 4, respectively. It can be seen that this investigation has been done for the PTSC equipped with a TCT and VGPR in 5 and 6 stages, respectively. Because as can be seen in Figure 2 in steps 1 to 3 and Fig.3 in steps 1 to 4 with the increase in the number of grid points, a solution independent of the grid has not yet been obtained, or in other words, the output solutions have high fluctuations. Therefore, in these cases, the number of grid points should be increased, and the process of reporting  $Nu_{ave}$  values should be compared with the previous cases. In other words, this process continues until reaching a solution independent of the grid. The presented results state that in the present problem, it is suitable for the PTSC along with the grid TCT with the number of 1664362 points and for the parabolic collector equipped with the VGPR grid with the number of 2304957 points.

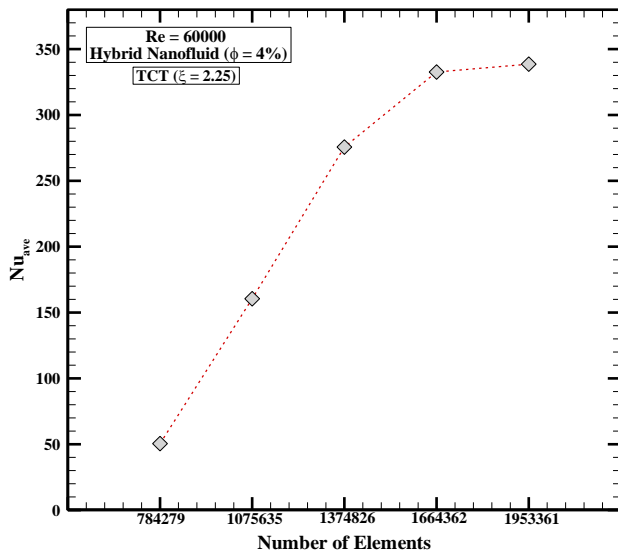


Fig. 3. The results obtained from the meshing in the AT along with the TCT

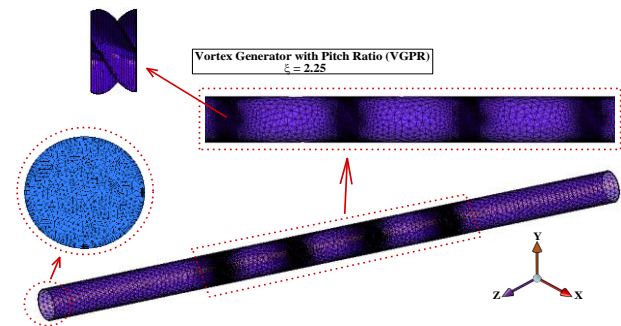
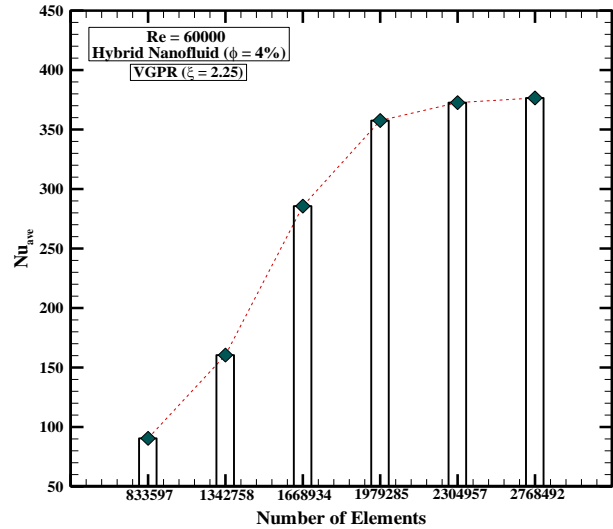


Fig. 4. The results obtained from the meshing in the AT along with the VGPR

#### Validation

Using the CFD technique, Shaker et al. [37] simulated a PTSC equipped with TT with different numbers. In addition, they used silver/aluminum oxide NF in this study. In order to ensure the numerical solution, validation was done with the study of Shaker et al. [37], and the results obtained from the displacement HT coefficient are compared in Fig. 5. It should be noted that the validation was done at different mass flow rates and different numbers of TT. The presented results are highly consistent. Therefore, you can be sure of the numerical solution and settings.

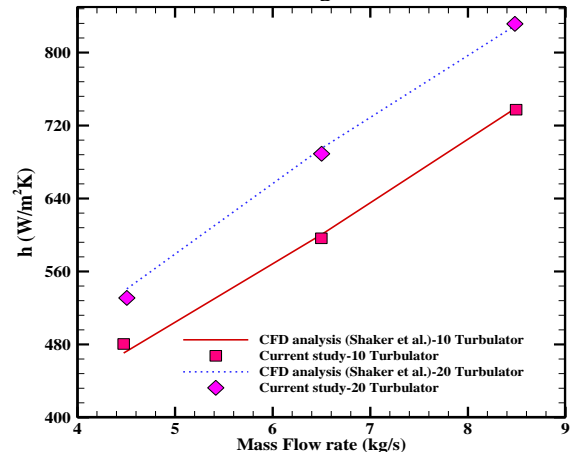


Fig. 5. Validation with reference [37]

**RESULTS AND DISCUSSION**

**Comparison of TP**

In this study, to investigate the efficiency of a VGPR and TCT, the results obtained from the  $Nu_{ave}$  in these two geometric modes have been compared. Fig. 6 compares the  $Nu_{ave}$  in a PTSC when using a VGPR and TCT. By observing the obtained results, increasing the speed change in the AT is known as a positive factor in all cases. Because in all these cases, the increase of this parameter has caused the  $Nu_{ave}$  to rise. In addition, Syltherm 800 BF has a lower  $k$  ratio than HNF Syltherm 800/DWCNT-GO, resulting in lower TP in PTSC. The lowest  $Nu_{ave}$  changes occur when the PTSC lacks a TCT and VGPR. Because their absence causes the flow to pass through the absorbent tube in a layered manner, and there are no specific changes in the flow behavior. This is even though the presence of a VGPR and TCT has intensified the changes in the  $Nu_{ave}$ . Because with the presence of these two mechanical parts, the TP also increases due to the mixing of the flow and the creation of vortices. As can be seen, using a VGPR compared to a TCT has made more changes in increasing the  $Nu_{ave}$ . This is because the way the VGPR are located at a suitable distance

from each other helps to increase the mixing rate and disturbance of the viscous layer. The use of VGPR causes a more significant growth in the heat transfer coefficient values compared to the TCT because, as is evident, the higher the speed of the HNF, the higher the heat transfer coefficient will be. In this study, the hybrid nanofluid flow speed will be high according to the assumption of a turbulent flow regime at high Reynolds numbers and the presence of VGPR. Therefore, this factor causes the heat transfer coefficient in the PTSC to increase, and as a result, the thermal performance increases. The images of the velocity contour in different states of the geometry of the VGPR and TCT are shown in Fig. 7. The pictures show that the main reason for the increase or decrease in speed in the AT is related to the presence or absence of the VGPR and TCT. Because when these mechanical parts are placed in the flow path of HNF Syltherm 800/DWCNT-GO, they change the shape of the flow lines and compress it. On the other hand, further investigation shows that another very influential factor in these contours is the geometrical change of the VGPR with the TCT (increasing the rotation rate of the blades).

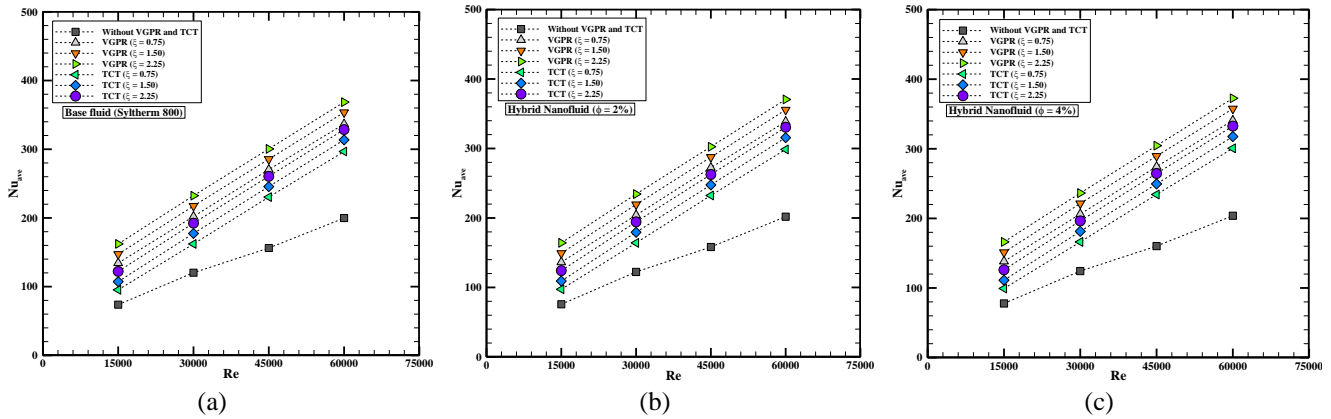
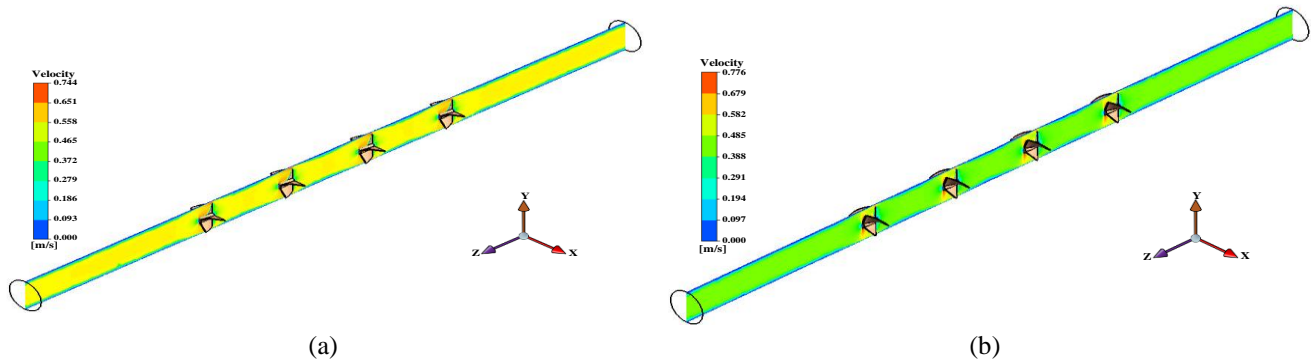


Fig. 6. Comparison of  $Nu_{ave}$  in PTSC when using VGPR and TCT



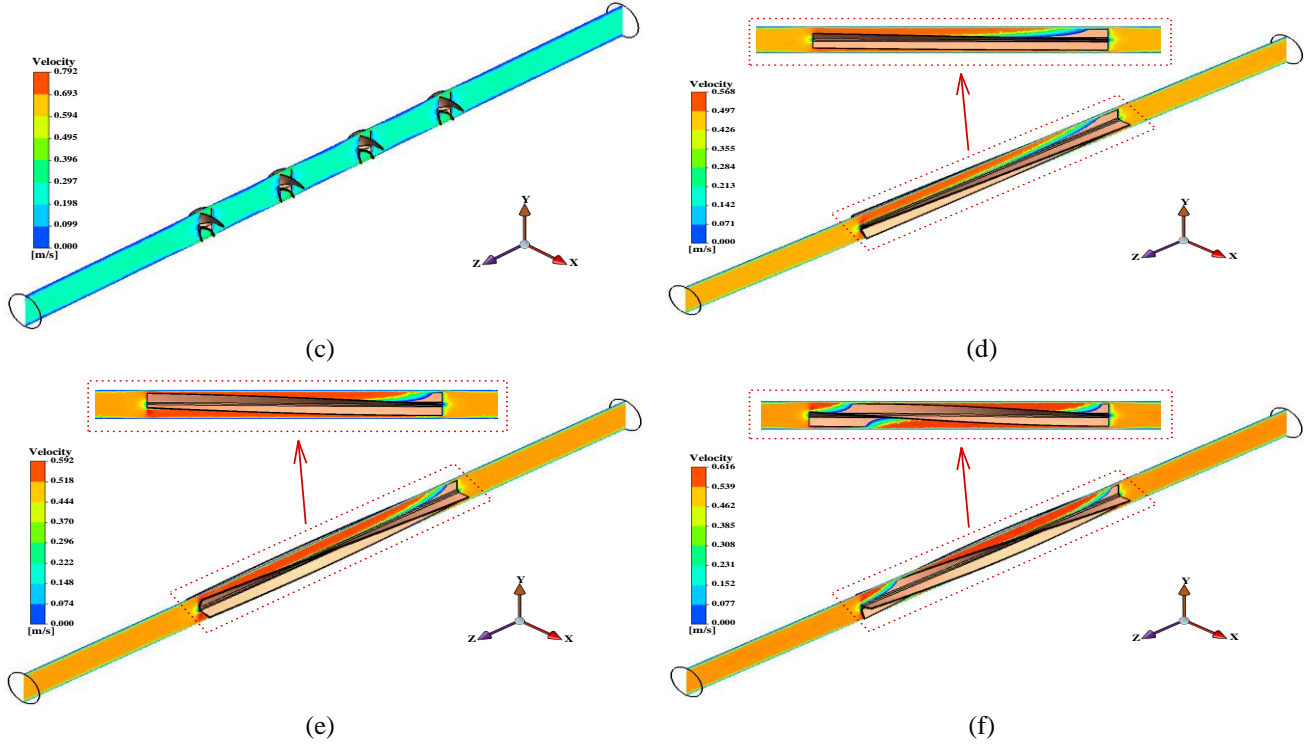


Fig. 7. Speed contour images for all geometric modes

**Comparison of Hydraulic Performance**

Designing engineering systems with optimal and low  $\Delta P$  has always been a concern of large engineering industries.  $\Delta P$  in engineering systems occurs due to various factors such as fluid viscosity, obstacles in the flow path, change of flow path, etc. Fig. 8 compares  $\Delta P$  in a PTSC when using a VGPR and TCT. By interpreting the output results, the most important factor in causing  $\Delta P$  is using a VGPR and TCT in the flow path inside the AT of the PTSC. Because, as the output results showed, when the AT is without a VGPR and

TCT, the  $\Delta P$  values do not change dramatically and are only affected by the  $Re$  and  $\phi$  are much less than in the case where the AT is equipped with a VGPR and TCT. Also, the amount of  $\Delta P$  created when using more VGPR is from the TCT because the geometry of the TCT is integrated and does not cause condensation of flow lines like the VGPR. In other words, placing the geometry of the VGPR at a certain distance in the flow path creates more rotating flow and larger eddies compared to the TCT.

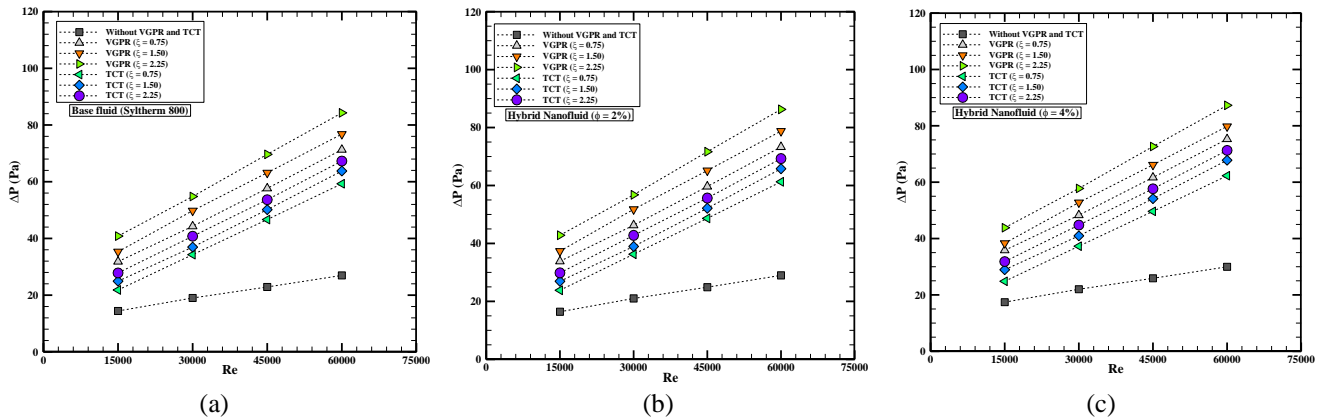


Fig. 8. Comparison of  $\Delta P$  in PTSC when using VGPR and TCT

The images of the pressure contour in different states of the geometry of the VGPR and TCT are shown in Fig. 9. By

inferring from the images provided from the numerical simulation output, it can be stated that the main reason for

the  $\Delta P$  in this problem is the presence of VGPR and TCT in the hybrid flow path of Syltherm 800/DWCNT-GO NF. Because when the VGPR and TCT are absent in the AT, the HNF flow will naturally follow a uniform path and have a lower  $\Delta P$ . However, the presence of a TCT and VGPR increases the  $\Delta P$  values to a great extent. Because the presence of VGPR and TCT prevents the flow of a HNF, the

$\Delta P$  reaches its maximum at the moment of impact. In addition, it is visible that the critical and influential factor in increasing the  $\Delta P$  is the geometrical deformation of the VGPR or TCT (increasing the rotation rate of the blades). Finally, referring to the pictures, it can be concluded that the  $\Delta P$  caused by VGPR s is more than TCT.

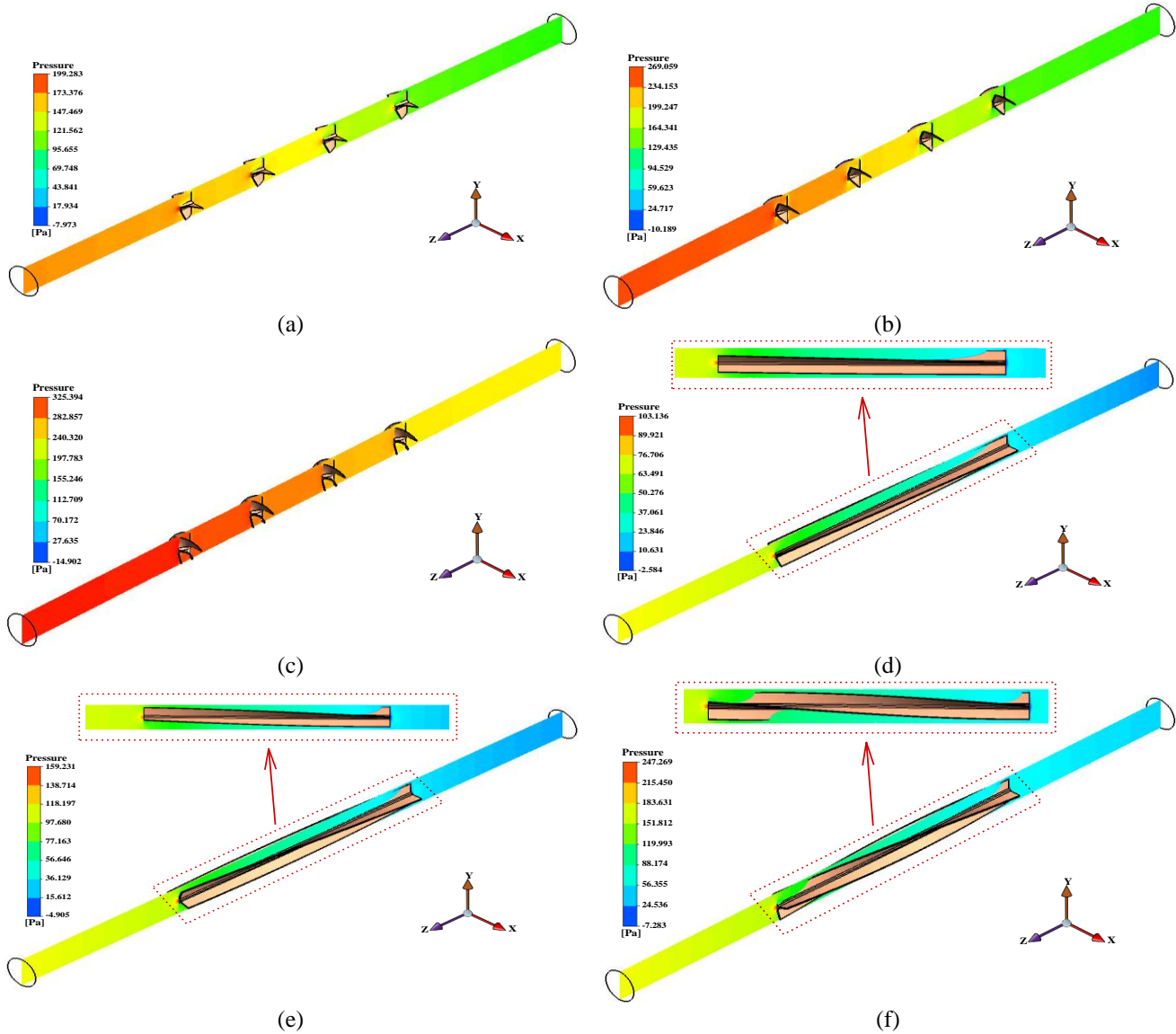


Fig. 9. Pressure contour images for all geometric modes

### PEC Index Comparison

The best method to check the hydrodynamic behavior of the fluid in computational fluid dynamics problems is to check the PEC index. Because by examining this parameter, we can conclude that adding a TCT or VGPR in the AT of the PTSC and changing its geometric parameters has a positive performance in the SS. Fig. 10 describes the results obtained from the comparison of the PEC index in the PTSC when using the VGPR and TCT. By interpreting the results, it can

be concluded that the addition of the TCT, VGPR and their geometrical change has a positive role in the hydrodynamic behavior of the HNF flow Syltherm 800 /DWCNT-GO. In all the geometric modes, the values obtained from the PEC index are greater than one, so it can be said that the use of these two mechanical parts always has better TP compared to the  $\Delta P$  obtained due to their presence. Also, by looking at the images related to the flow lines in Fig. 11, it can be stated that the presence of VGPR and TCT causes the rotation of

the Syltherm 800/DWCNT-GO HNF flow. Because the images related to these contours clearly show the density of HNF Syltherm 800/ DWCNT-GO due to collision with VGPR and TCT. Finally, according to the pictures, it can be seen that the presence of VGPR has caused more swirling flow than TCT. No matter how high the thermal efficiency is in the PTSC, it saves energy and makes it economically viable. Therefore, increasing the thermal efficiency of the solar system in the present study through VGPR, TCT, and hybrid nanofluid is always known as a positive factor. As the output results show, using these three factors has always had a positive effect on the growth of the heat transfer coefficient. Therefore, VGPR have better thermal performance than TCT.

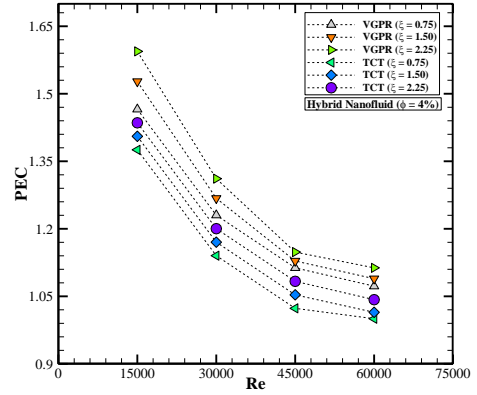


Fig. 10. Comparison of PEC index in PTSC when using VGPR and TCT

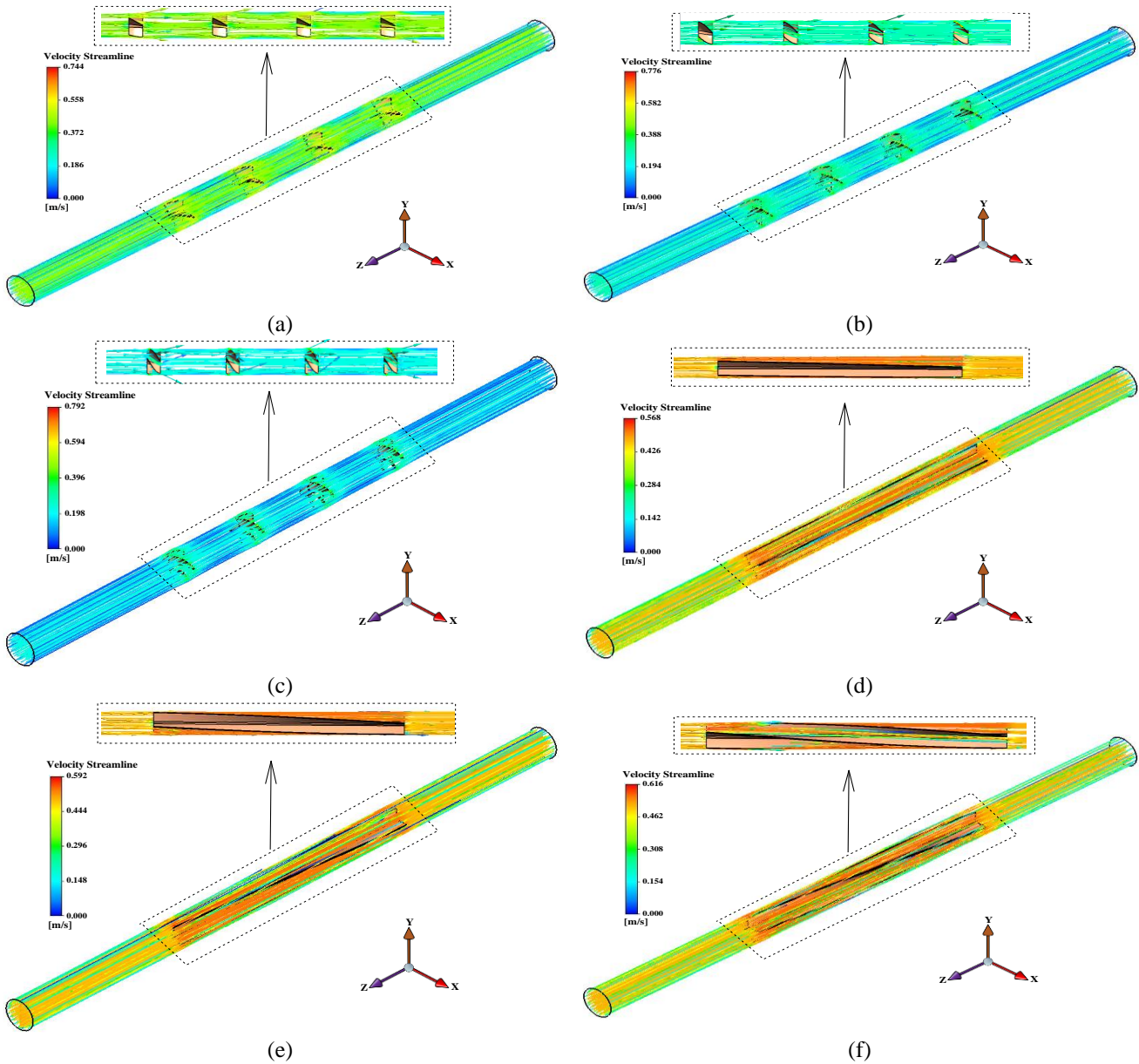


Fig. 11. contour images of flow lines for all geometric modes

### Comparison of $\eta_{en}$

Renewable energy is vital for the future of the world. The main reason for this is the environmental issues caused by the current methods of energy production. On the other hand, energy has a special place in the world community, and we must make intelligent choices to prevent environmental disasters, severe energy shortages, and even social chaos or war. A renewable energy source is a natural and continuous flow of energy in the surrounding environment. Therefore, calculating the  $\eta_{en}$  of SS is of great importance. The values obtained from the comparison of  $\eta_{en}$  in a PTSC when using a VGPR and TCT are presented in Fig. 12. By interpreting the results, all the parameters examined in this numerical simulation affect the  $\eta_{en}$  values. In other words, the increase in Re and  $\phi$  has increased the  $\eta_{en}$  values in the SS. However, the values of  $\eta_{en}$  based on the geometrical change of the VGPR and TCT are higher than the Re and  $\phi$  changes. It can be stated that the use of VGPR, turbulators, and hybrid nanofluid has increased the potential of a certain amount of energy in the solar collector. Therefore, this factor has increased the energy efficiency of the PTSC. The presented

results state that using the VGPR compared to the TCT creates a higher  $\eta_{en}$  in the SS. Eddy viscosity contour images in different states of the geometry of the VGPR and TCT are shown in Fig. 13. By examining the images, the amount of eddy viscosity changes along the length of the AT is affected by the presence of the VGPR and TCT. Because when there is no VGPR and TCT in the flow path, the eddy viscosity contour will naturally be unchanged. By examining the presented images, the higher the eddy viscosity of Bitsher, the higher the fluctuation and mixing of the flow will be. As a result, the TP will be higher. The presence of a VGPR and TCT in the flow path significantly helps to increase the values of eddy viscosity and TP. Therefore, referring to the pictures, VGPR have a much more favorable role than circulators in changing the shape of flow lines, creating a swirling flow, and increasing viscosity. It can be stated that, the amount of viscosity changes in the areas close to the VGPR is more significant than that of the TCT. Because the arrangement of the VGPR at a certain distance has caused the NF flow to start rotating between the empty spaces between them, this is one of the reasons for the TP of these mechanical parts rather than TCT.

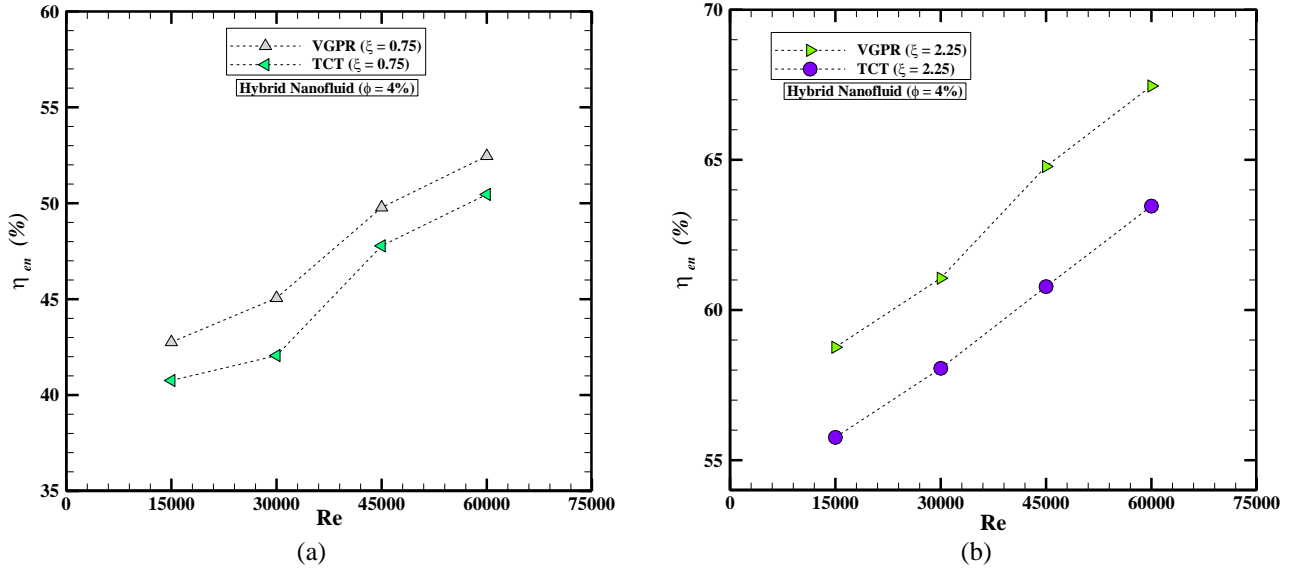
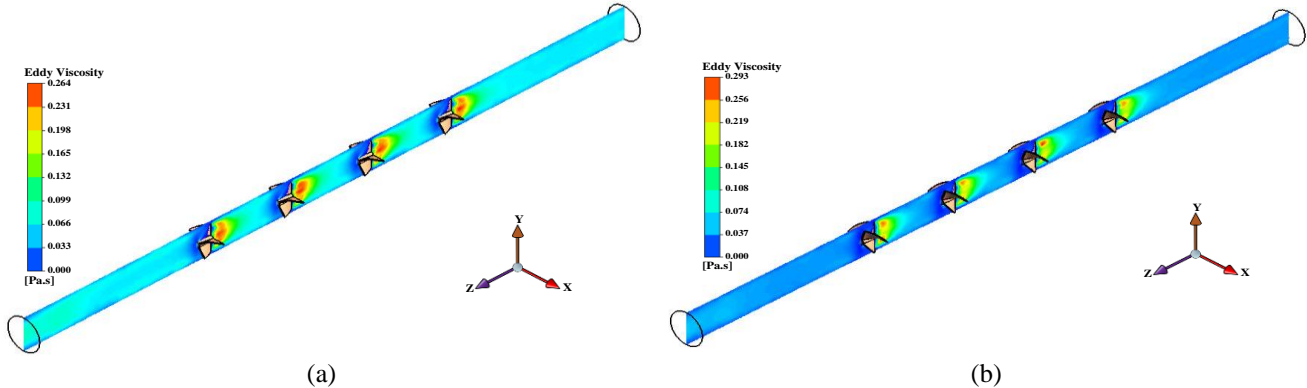


Fig. 12. Comparison of  $\eta_{en}$  in PTSC when using VGPR and TCT



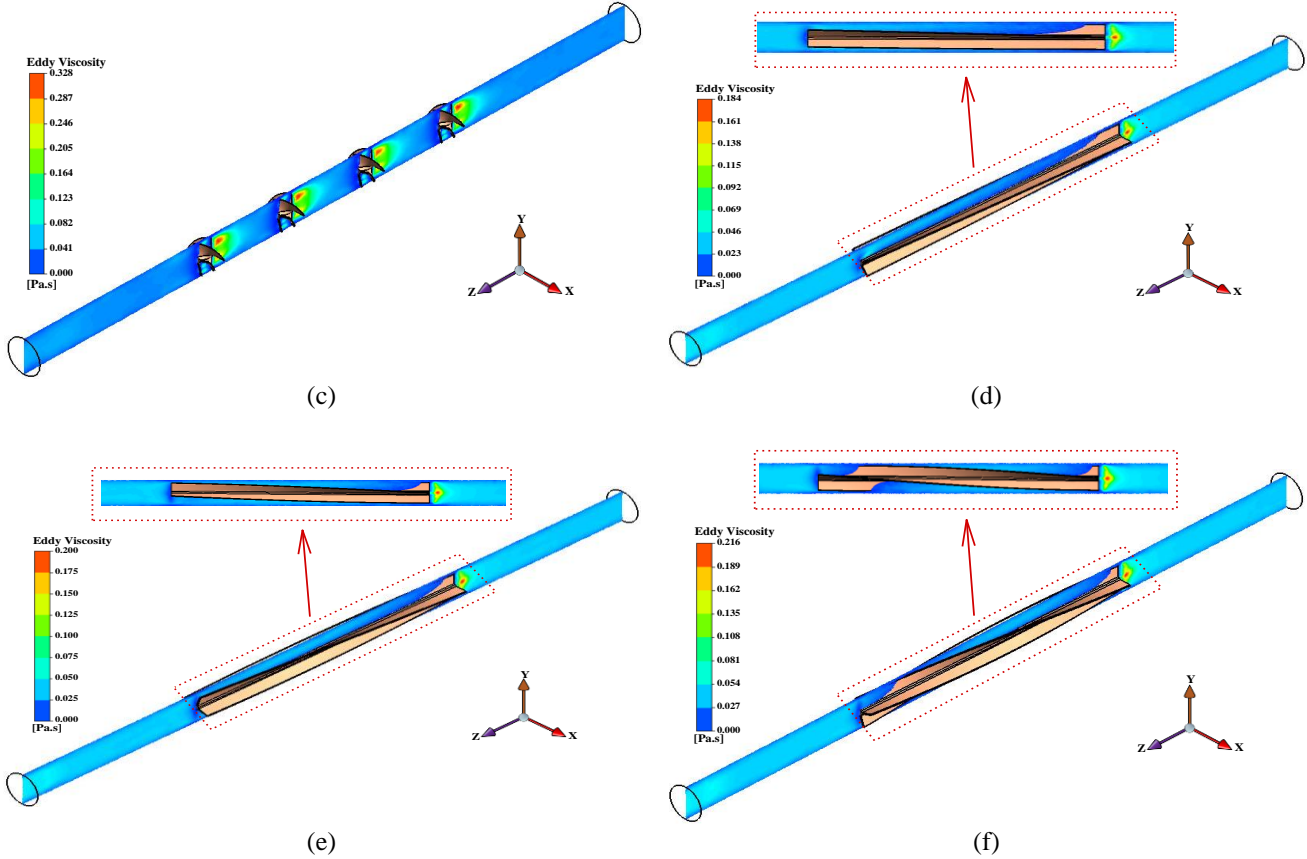


Fig. 13. Eddy viscosity contour images for all geometric modes

### Comparison of $\eta_{ex}$

The growth of energy demand in recent decades has caused problems such as environmental problems and lack of resources and fuel, so finding solutions to increase efficiency in energy production is more critical than ever. Increasing energy efficiency causes a reduction in fuel consumption and the reduction of pollutants caused by it. One of the ways to increase energy efficiency is exergy analysis and understanding the irreversibility factors of systems. Also, by combining exergy and economical methods, it is possible to design the optimal state of heating and power generation systems. The values obtained from comparing the  $\eta_{ex}$  in the PTSC when using the VGPR and the TCT are displayed as a diagram in Fig. 14. By interpreting the results, all the parameters examined in this numerical simulation affect the  $\eta_{ex}$  values. However, the amount of change in  $\eta_{ex}$  based on the geometrical change of the VGPR and TCT is more than Re changes and  $\phi$ .  $\eta_{ex}$  is the maximum amount of work that

can be obtained from an ideal system, given the amount of applied energy. In other words,  $\eta_{ex}$  flow is a valuable amount of energy in any process that can be converted into practical work. For this reason, it can be used as one of the criteria for optimizing energy systems. In this numerical simulation, using a VGPR is more suitable than a TCT regarding  $\eta_{ex}$ . Because as was explained before, by examining the  $\eta_{ex}$ , it was observed that the maximum practical work received from the SS was obtained when using the VGPR in the flow path of HNF Syltherm 800/DWCNT-GO. Finally, the maximum amount of work that can be obtained from the PTSC is when using VGPR. Because the amount of applied energy is higher, in other words, exergy flow is a valuable amount of energy in any process that can be converted into practical work. For this reason, it can be used as one of the criteria for optimizing energy systems.

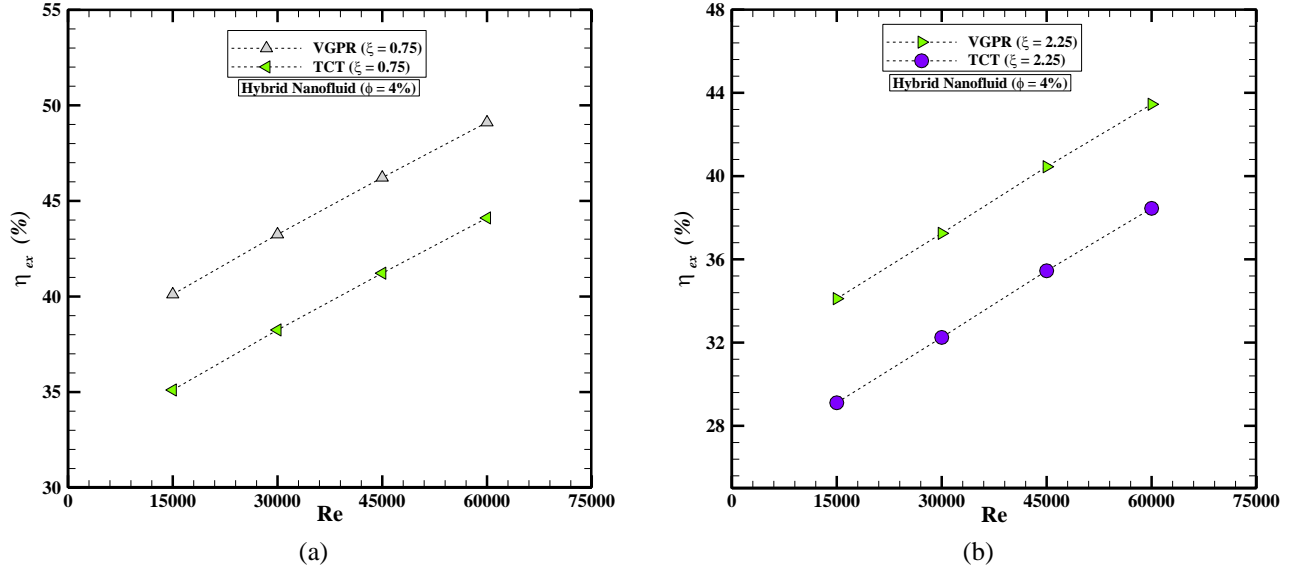


Fig. 14. Comparison of  $\eta_{ex}$  in PTSC when using VGPR and TCT

## CONCLUSION

The present study follows a 3D modeling of the geometry of a PTSC equipped with a TCT and a VGPR, considering the FVM to solve the governing equations. The AT of this PTSC is equipped with a TCT and VGPR in order to increase TP. Also, the efficiency of their use on different output parameters have been compared. In addition, in order to be more practical, the efficiency of the geometric shape of the TCT and VGPR on various parameters in the output has been investigated. In order to make the study more practical, GO and DWCNT NP are dispersed in this BF. The study is conducted at high Re (from 15,000 to 60,000), corresponding to the turbulent regime's range. The numerical simulation results show that:

- In all cases, the increase in the velocity changes in the AT is a positive factor. Because in all these cases, the increase of this parameter has caused the  $Nu_{ave}$  to rise.
- Syltherm 800 BF has a lower  $k$  in the PTSC due to its lower  $k$  ratio than HNF Syltherm 800/DWCNT-GO.
- The lowest  $Nu_{ave}$  changes occur when the PTSC lacks a TCT and VGPR. Because their absence causes the flow to pass through the absorbent tube in a layered manner, and there are no specific changes in the flow behavior.
- The presence of VGPR and TCT has intensified the changes in the  $Nu_{ave}$ . Because with the presence of these

two mechanical parts, the TP also increases due to the mixing of the flow and the creation of vortices. This is because the way the VGPR s are located at a suitable distance from each other helps to increase the mixing rate and disturbance of the viscous layer.

- The addition of TCT, VGPR, and their geometrical change has a positive role in the hydrodynamic behavior of Syltherm 800/DWCNT-GO HNF flow. In all the geometric modes, the values obtained from the PEC index are more significant than one, so using these two mechanical parts always has better TP than the  $\Delta P$  obtained due to their presence.
- The increase in Re and  $\phi$  has increased the  $\eta_{en}$  values in the SS. However, the values of  $\eta_{en}$  based on the geometrical change of the VGPR and TCT are more than the Re and  $\phi$  changes.
- The presented results state that using the VGPR compared to the TCT creates a higher  $\eta_{en}$  in the SS.
- By examining the  $\eta_{ex}$ , it was observed that the maximum practical work received from the SS was obtained when using the VGPR in the flow path of HNF Syltherm 800/DWCNT-GO.

## REFERENCES

- [1] Göksu TT, Behçet R. Experimental investigation of the effect of a novel curved winglet vortex generator on heat transfer with a designed controller circuit. *International Journal of Thermal Sciences*. 2022 Oct 1;180:107724.
- [2] Parsaiemehr M, Pourfattah F, Akbari OA, Toghraie D, Sheikhzadeh G. Turbulent flow and heat transfer of Water/Al<sub>2</sub>O<sub>3</sub> nanofluid inside a rectangular ribbed channel. *Physica E: Low-Dimensional Systems and Nanostructures*. 2018 Feb 1;96:73-84.
- [3] Larki AJ, Ghafouri A, Assareh E, Moravej M. Investigation of the effects of the detachable vortex generators series on phase change material behavior in an energy storage system. *Journal of Building Engineering*. 2022 Jul 15;52:104384.
- [4] Jassim EI, Ahmed F. Assessment of nanofluid on the performance and energy-environment interaction of Plate-Type-Heat exchanger. *Thermal Science and Engineering Progress*. 2021 Oct 1;25:100988.
- [5] Sun Z, Chen Q, Zheng N. Experimental and numerical studies of intensified turbulent heat transfer in round pipes with curved wing vortex generators. *International Journal of Heat and Mass Transfer*. 2021 Dec 1;180:121823.
- [6] Abidi A, El-Shafay AS, Degani M, Guedri K, Sajadi SM, Sharifpur M. Improving the thermal-hydraulic performance of parabolic solar collectors using absorber tubes equipped with perforated twisted tape containing nanofluid. *Sustainable Energy Technologies and Assessments*. 2022 Aug 1;52:102099.
- [7] Sheikholeslami M. Numerical investigation of solar system equipped with innovative turbulator and hybrid nanofluid. *Solar Energy Materials and Solar Cells*. 2022 Aug 15;243:111786.
- [8] Modi AJ, Rathod MK. Comparative study of heat transfer enhancement and pressure drop for fin-and-circular tube compact heat exchangers with sinusoidal wavy and elliptical curved rectangular winglet vortex generator. *International Journal of Heat and Mass Transfer*. 2019 Oct 1;141:310-26.
- [9] Sharma AK, Vishwakarma DK, Mukherjee S, Bhattacharyya S. Computational Investigation on Flow Dynamics and Heat Transfer of Nanofluid in Low Reynolds Number Under Magnetic Field. In *Conference on Fluid Mechanics and Fluid Power 2021 Dec 27* (pp. 631-635). Singapore: Springer Nature Singapore. [https://doi.org/10.1007/978-981-19-6270-7\\_105](https://doi.org/10.1007/978-981-19-6270-7_105).
- [10] Ye M, Du J, Wang J, Chen L, Varbanov PS, Klemeš JJ. Investigation on thermal performance of nanofluids in a microchannel with fan-shaped cavities and oval pin fins. *Energy*. 2022 Dec 1;260:125000.
- [11] Das AK, Hiremath SS. Investigation on the thermohydraulic performance and entropy-generation of novel butterfly-wing vortex generator in a rectangular microchannel. *Thermal Science and Engineering Progress*. 2022 Dec 1;36:101531.
- [12] Liang X, Kumar NB, Mansir IB, Singh PK, Abed AM, Dahari M, Nasr S, Albalawi H, Cherif A, Wae-hayee M. Management of heat transfer and hydraulic characteristics of a micro-channel heat sink with various arrangements of rectangular vortex generators utilizing artificial neural network and response surface methodology. *Case Studies in Thermal Engineering*. 2023 Apr 1;44:102850.
- [13] Sheikholeslami M, Farshad SA. Investigation of solar collector system with turbulator considering hybrid nanoparticles. *Renewable Energy*. 2021 Jun 1;171:1128-58.
- [14] Al-Rashed AA, Alnaqi AA, Alsarraf J. Thermo-hydraulic and economic performance of a parabolic trough solar collector equipped with finned rod turbulator and filled with oil-based hybrid nanofluid. *Journal of the Taiwan Institute of Chemical Engineers*. 2021 Jul 1;124:192-204.
- [15] Bellos E, Tzivanidis C, Tsimpoukis D. Enhancing the performance of parabolic trough collectors using nanofluids and turbulators. *Renewable and Sustainable Energy Reviews*. 2018 Aug 1;91:358-75.
- [16] Gururatana S, Prapainop R, Chuepeng S, Skullong S. Development of heat transfer performance in tubular heat exchanger with improved NACA0024 vortex generator. *Case Studies in Thermal Engineering*. 2021 Aug 1;26:101166.
- [17] Zheng D, Du J, Wang W, Klemeš JJ, Wang J, Sundén B. Analysis of thermal efficiency of a corrugated double-tube heat exchanger with nanofluids. *Energy*. 2022 Oct 1;256:124522.
- [18] Berber A, Guerdal M. Estimation of forced heat convection in a rectangular channel with curved-winglet vortex generator: A machine learning approach. *Thermal Science and Engineering Progress*. 2023 Jan 1;37:101563.
- [19] Lu G, Zhai X. Analysis on heat transfer and pressure drop of fin-and-oval-tube heat exchangers with tear-drop delta vortex generators. *International Journal of Heat and Mass Transfer*. 2018 Dec 1;127:1054-63.
- [20] Nikoozadeh A, Behzadmehr A, Payan S. Numerical investigation of turbulent heat transfer enhancement using combined propeller-type turbulator and nanofluid in a circular tube. *Journal of Thermal Analysis and Calorimetry*. 2020 May;140:1029-44. <https://doi.org/10.1007/s10973-019-08578-x>.
- [21] Mohammed HA, Vuthaluru HB, Liu S. Heat transfer augmentation of parabolic trough solar collector receiver's tube using hybrid nanofluids and conical turbulators. *Journal of the Taiwan Institute of Chemical Engineers*. 2021 Aug 1;125:215-42.
- [22] Fuxi S, Sina N, Sajadi SM, Mahmoud MZ, Abdelrahman A, Aybar HŞ. Artificial neural network

- modeling to examine spring turbulators influence on parabolic solar collector effectiveness with hybrid nanofluids. *Engineering Analysis with Boundary Elements*. 2022 Oct 1;143:442-56.
- [23] Alqaed S, Mustafa J, Sharifpur M, Alharthi MA. Numerical simulation and artificial neural network modeling of exergy and energy of parabolic trough solar collectors equipped with innovative turbulators containing hybrid nanofluids. *Journal of Thermal Analysis and Calorimetry*. 2023 Aug;148(16):8611-26. <https://doi.org/10.1007/s10973-022-11538-7>.
- [24] Song K, Hu D, Zhang Q, Zhang K, Wu X, Wang L. Thermal-hydraulic characteristic of a novel wavy fin-and-circle tube heat exchanger with concave curved vortex generators. *International Journal of Heat and Mass Transfer*. 2022 Sep 15;194:123023.
- [25] Aghaei A, Dezfulizadeh A, Fadaei Dehar A, Sepehrirad M, Mazaheri H. Determination of energy efficiency and exergy of solar collector bed, operating plate under turbulent nanoscale flow with molybdenum disulfide nanoparticles in different morphologies for tropical regions of Iran. *Energy Engineering and Management*. 2023 Jan 29;12(1):130-43.
- [26] Razzaghi MJ, Asadollahzadeh M, Tajbakhsh MR, Mohammadzadeh R, Abad MZ, Nadimi E. Investigation of a temperature-sensitive ferrofluid to predict heat transfer and irreversibilities in LS-3 solar collector under line dipole magnetic field and a rotary twisted tape. *International Journal of Thermal Sciences*. 2023 Mar 1;185:108104.
- [27] Roohi R, Arya A, Akbari M, Amiri MJ. Performance evaluation of an absorber tube of a parabolic trough collector fitted with helical screw tape inserts using CuO/industrial-oil nanofluid: a computational study. *Sustainability*. 2023 Jul 5;15(13):10637. <https://doi.org/10.3390/su151310637>.
- [28] Dezfulizadeh A, Aghaei A, Sheikhzadeh GA. Comprehensive 3E analyses of a parabolic trough collector equipped with an innovative combined twisted turbulator. *Engineering Analysis with Boundary Elements*. 2023 May 1;150:507-27.
- [29] Esmaili Z, Akbarzadeh S, Rashidi S, Valipour MS. Effects of hybrid nanofluids and turbulator on efficiency improvement of parabolic trough solar collectors. *Engineering Analysis with Boundary Elements*. 2023 Mar 1;148:114-25.
- [30] Abidi A. Improving the efficiency of parabolic solar collector (PSC) containing magnetic nanofluid with absorber pipe equipped with square twisted turbulator. *Sustainable Energy Technologies and Assessments*. 2022 Aug 1;52:102083.
- [31] Jafaryar M, Sheikholeslami M. Efficacy of turbulator on performance of parabolic solar collector with using hybrid nanomaterial applying numerical method. *Renewable Energy*. 2022 Oct 1;198:534-48.
- [32] Shirazi M, Shateri A, Bayareh M. Numerical investigation of mixed convection heat transfer of a nanofluid in a circular enclosure with a rotating inner cylinder. *Journal of Thermal Analysis and Calorimetry*. 2018 Aug;133:1061-73. <https://doi.org/10.1007/s10973-018-7186-y>.
- [33] Shiriny A, Bayareh M, Ahmadi Nadooshan A, Bahrami D. Forced convection heat transfer of water/FMWCNT nanofluid in a microchannel with triangular ribs. *SN Appl Sci*. 2019; 1 (12): 1631. <http://doi.org/10.1007/s42452-019-019-7>. <https://doi.org/10.1007/s42452-019-1678-7>.
- [34] Bahrami D, Bayareh M. Impacts of channel wall twisting on the mixing enhancement of a novel spiral micromixer. *Chemical Papers*. 2022 Jan 1:1-2. <https://doi.org/10.1007/s11696-021-01876-5>.
- [35] Bayareh M, Pordanjani AH, Nadooshan AA, Dehkordi KS. Numerical study of the effects of stator boundary conditions and blade geometry on the efficiency of a scraped surface heat exchanger. *Applied Thermal Engineering*. 2017 Feb 25;113:1426-36.
- [36] Sepyani M, Shateri A, Bayareh M. Investigating the mixed convection heat transfer of a nanofluid in a square chamber with a rotating blade. *Journal of Thermal Analysis and Calorimetry*. 2019 Jan 14;135:609-23. <https://doi.org/10.1007/s10973-018-7098-x>.
- [37] Shaker B, Gholinia M, Pourfallah M, Ganji DD. CFD analysis of Al<sub>2</sub>O<sub>3</sub>-syltherm oil Nanofluid on parabolic trough solar collector with a new flange-shaped turbulator model. *Theoretical and Applied Mechanics Letters*. 2022 Feb 1;12(2):100323. <https://doi.org/10.1016/j.taml.2022.100323>.
- [38] ANSYS I. Ansys Academic Research, Release 18.1. In *Advanced Analysis Guide, Coupled Field Analysis Guide, Release 17.1 Doc 2017*. Ansys.
- [39] Typical Properties of SYL THERM 800 Fluid 1. n.d.
- [40] Labib MN, Nine MJ, Afrianto H, Chung H, Jeong H. Numerical investigation on effect of base fluids and hybrid nanofluid in forced convective heat transfer. *International Journal of Thermal Sciences*. 2013 Sep 1;71:163-71.
- [41] Rahimi A, Kasaeipoor A, Malekshah EH, Kolsi L. Experimental and numerical study on heat transfer performance of three-dimensional natural convection in an enclosure filled with DWCNTs-water nanofluid. *Powder technology*. 2017 Dec 1;322:340-52. <https://doi.org/10.1016/j.powtec.2017.09.008>.
- [42] Sundar LS, Singh MK, Ferro MC, Sousa AC. Experimental investigation of the thermal transport properties of graphene oxide/Co<sub>3</sub>O<sub>4</sub> hybrid nanofluids. *International Communications in Heat and Mass Transfer*. 2017 May 1;84:1-0.
- [43] Aliehyaei M, Joshaghani AH, Najafizadeh MM. Energy, exergy, economic and environmental analysis of parabolic trough collector containing hybrid

- nanofluid equipped with turbulator. *Engineering Analysis with Boundary Elements*. 2023 May 1;150:492-506.  
<https://doi.org/10.1016/j.enganabound.2023.02.031>.
- [44] Khetib Y, Alahmadi A, Alzaed A, Sharifpur M, Cheraghian G, Siakachoma C. Simulation of a parabolic trough solar collector containing hybrid nanofluid and equipped with compound turbulator to evaluate exergy efficacy and thermal-hydraulic performance. *Energy Science & Engineering*. 2022 Nov;10(11):4304-17. <https://doi.org/10.1002/ese3.975>
- [45] Aghaei A, Enayati M, Beigi N, Ahmadi A, Pourmohamadian H, Sadeghi S, Dezfulizadeh A, Golzar A. Comparison of the effect of using helical strips and fins on the efficiency and thermal–hydraulic performance of parabolic solar collectors. *Sustainable Energy Technologies and Assessments*. 2022 Aug 1;52:102254.